

# A comparative study for shear strengthening techniques of reinforced concrete beams using FRP

A. M. Morsy, N. H. El-Ashkar & K. M. Helmi

*Construction & Building Engineering Department*

*Arab Academy for Science, Technology & Maritime Transport, Alexandria, Egypt*

**ABSTRACT:** This paper presents the results of a pilot testing program that was undertaken to study the feasibility of strengthening RC beams in shear using FRP reinforcement internally embedded in holes drilled through the depth of the beam. Five similar beams were tested in this program, a control beam without strengthening, and three beams strengthened using externally bonded CFRP sheets, NSM CFRP strips and embedded CFRP and GFRP rods. The specimens strengthened with externally bonded sheets and internally embedded CFRP reinforcement had a 30% increase in their shear capacity while the specimens strengthened with NSM strips and internally embedded GFRP reinforcement had a 60% increase in their shear capacity, compared to the control specimens. The results thus confirm the feasibility of the proposed technique.

## 1 INTRODUCTION

Strengthening Reinforced Concrete (RC) structures with Fiber Reinforced Polymers (FRP) has been studied and successfully implemented in field applications since the early 1990's. In addition to the superior properties of FRP, such as high strength to weight ratios and corrosion resistance, strengthening RC structures with FRP in most cases is easier and requires less labour and time than conventional materials. FRP has been used in strengthening RC columns and beams both in flexure and in shear. For the strengthening of RC beams in shear, typically carbon or glass fiber sheets are externally bonded to the sides or the sides and bottom of RC beams forming a U wrap using an epoxy adhesive. Another method for strengthening RC members with FRP is the Near surface mounting (NSM) technique, where grooves are cut in the concrete cover and FRP rods or thin plates referred to as strips are installed inside these grooves and bonded using an epoxy adhesive. Strengthening RC beams in shear with FRP round rods was studied by De Lorenzis & Nanni, (2001), Rizzo & De Lorenzis (2009), and Tanarlan, (2011), while Barros & Dias (2006), Rizzo & De Lorenzis (2009) and Dias & Barros (2010) studied strengthening RC beams in shear with CFRP strips. For the NSM technique the amount of site installation work may be reduced, as surface preparation other than grooving is no longer required e.g., plaster removal is not necessary; irregularities of the concrete surface can be more easily accommodated. Additionally

the FRP is protected by the concrete cover and therefore is less prone to accidental damage and vandalism (De Lorenzis & Teng 2007). Furthermore the studies by Rizzo & De Lorenzis (2009) and Dias & Barros (2010) have shown that shear strengthening of RC beams using the NSM technique is more efficient than using the externally bonded technique. However the amount of FRP that could be used with the NSM technique is limited by the concrete cover available to accommodate the grooves. Additionally there is the possibility of damaging the main reinforcement during cutting the grooves due to the lack of proper concrete cover resulting from the misplacement of the reinforcement during construction.

The authors therefore suggest another technique for strengthening RC beams in shear, where holes are drilled through the depth of the beam and then FRP round bars are embedded in the holes using epoxy adhesive. This technique has the same advantage as the NSM technique; in addition the embedment of the FRP bars inside the beams will improve the aesthetics since there will be no surface grooves on the sides of the beam. The presence of the reinforcement inside the beam may also improve the bond behavior of this system due to the confinement effect

The details and results of a pilot test program that was undertaken to examine the feasibility of this technique are presented in the following sections.

## 2 EXPERIMENTAL PROGRAM

Five specimens were tested in this program, a control specimen, and four specimens strengthened using three different techniques. The following is a description of the specimens and the materials used.

### 2.1 Description of the beams

Five reinforced concrete beams were tested in this program. The specimens had a cross section of 160 mm x 300 mm, and a total length of 2.40 meters. The specimens were designed to fail in shear at one side (The weak side). For flexure reinforcement, four 22 mm deformed bars arranged in two layers were used as bottom reinforcement, while two 22 mm deformed bars were used as top reinforcement. The shear reinforcement for the strong side consisted of 10 mm stirrups spaced at 50 mm, while the shear reinforcement for the weak side consisted of 6 mm bars with a spacing of 150 mm. Figure 1 shows the reinforcement details of the beams.

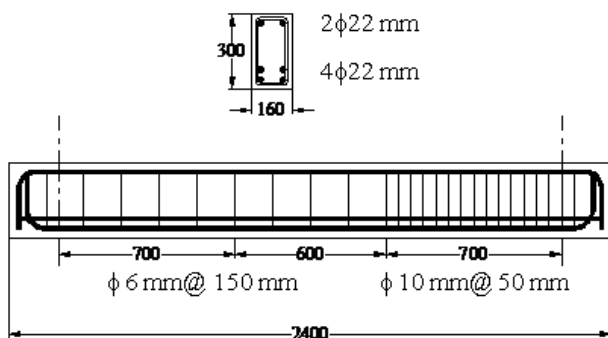


Figure 1 Reinforcement details of the specimens

### 2.2 Test specimens

Five identical beams constructed as mentioned in the previous section were tested in this program. The first specimen "Control" was a control specimen without any strengthening. The second specimen "EB" was strengthened in shear using CFRP sheets externally bonded to the sides and bottom of the beam forming a U wrap. A single layer of 60 mm wide sheets with a spacing of 150 mm was used to strengthen this specimen. Figure 2 shows the strengthening of the EB specimen. The third specimen "NSM" was strengthened in shear using NSM CFRP laminates mounted inside grooves cut in the concrete cover of both sides of the beams. 1.2 x 15 mm strips with a spacing of 75 mm were used to strengthen this specimen. Figures 3 and 4 illustrate the strengthening of specimen NSM. The fourth and fifth specimens "IER-G" and "IER-C" were strengthened using 12 mm Glass and Carbon FRP bars embedded in circular holes drilled through the depth of the beams respectively. All the bars had a spacing of 150 mm.

Figures 5 to 7 show the preparation work for specimen IER-G. The configuration of the specimens was chosen so all specimens would have an equal amount of material. Table 1 provides a summary of the details of the specimens used in this program.

Table 1 Specimen details

Specimen	Strengthening Technique	Material	Dimensions of material	Spacing
Control	None			
EB	Externally bonded sheets	CFRP	60 mm wide sheets (One Layer)	150 mm
NSM	Near surface mounted strips	CFRP	1.2 X 15 mm strips	75 mm
IER-C	Internally embedded reinforcement	CFRP	12 mm Bars	150 mm
IER-G	Internally embedded reinforcement	GFRP	12 mm Bars	150 mm

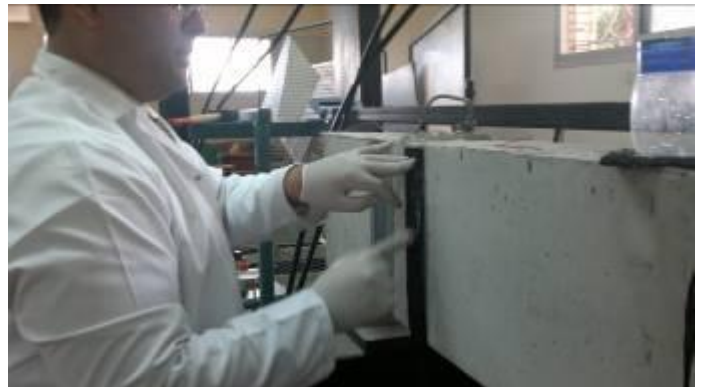


Figure 2 Strengthening of specimen EB



Figure 3 Cutting grooves for specimen NSM



Figure 4 Installing FRP strips in specimen NSM



Figure 5 Drilling of holes for specimen IER-G



Figure 6 Installing of reinforcement in specimen IER-G

### 2.3 Material properties

The concrete used in these tests had a strength of 20 MPa based on testing 100 mm cubes. The steel bars used for the flexure reinforcement and the stirrups on the strong side had a nominal yield strength of 360 MPa, while the bars used for reinforcing the weak side had a nominal yield strength of 240 MPa. Sikawrap 230 C carbon fiber sheets were used for the EB specimen. 1.2 mm thick MBrace S&P CFRP laminates manufactured by BASF were used for the

NSM specimen. 12 mm V-Rod FRP bars manufactured by Pultral Inc. were used for IER specimens. Sikadur 330 epoxy adhesive was used for the CFRP sheets while Sikadur 31 CF epoxy adhesive was used for all the other specimens.

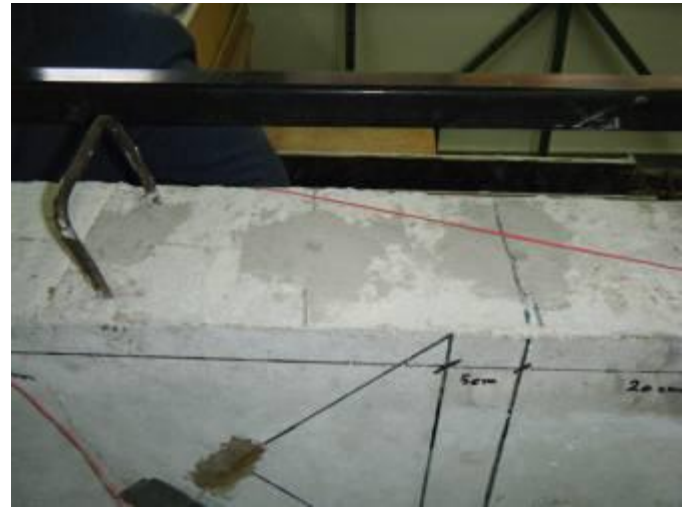


Figure 7 Specimen IER-G after strengthening

### 2.4 Test setup and instrumentation

All specimens were tested under four point bending. The span of the beams was 2.0 m and the distance between the loads was 0.6 m. The shear span for both sides was 0.7 m which is larger than 2.5 times the depth of the beam to avoid effects of arching action. Three dial gauges were used to measure the deflection at midspan, and both loading points. A strain gauge was mounted on the second stirrups after the support at the weak side. Long strain gauges were also mounted on the concrete surface at a 45° angle as shown in Figure 9. In addition strain gauges were also mounted on the second sheet, laminate and bar after the support for specimens EB, NSM and IER-C respectively. Loading was applied manually through a hydraulic pump to two hydraulic jacks at increments of 10 kN, at which time readings from the dial gauges and strains were manually recorded. Figures 8 and 9 show the test setup for the specimens.

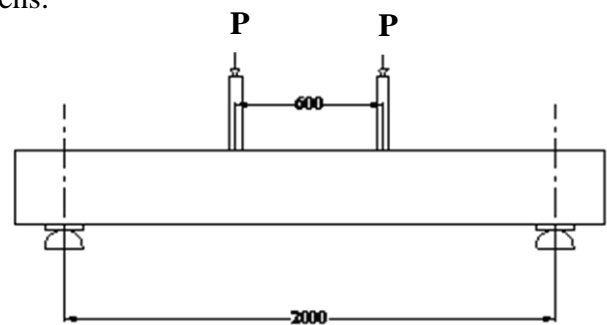


Figure 8 Test setup

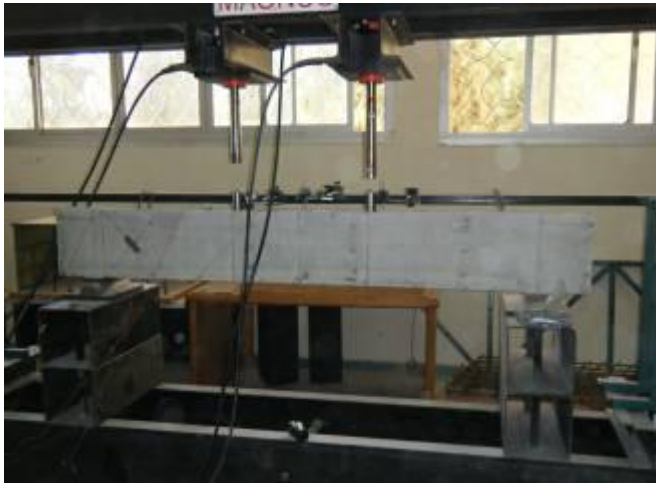


Figure 9 Test setup



Figure 10 Crack pattern of control specimen

### 3 TEST RESULTS

#### 3.1 Specimens' behavior and failure modes

All specimens failed in shear and all of the strengthened beams failed due to debonding. The following sections provide a description of the specimens' behavior during testing. Table 2 presents a summary of the test results "the loads for one jack only".

Table 2 Failure and first crack loads

Specimen	First crack load (kN)	Failure load (kN)
Control	70	100
EB	78	130
NSM	80	155
IER-C	70	138
IER-G	70	160

##### 3.1.1 Control specimen

For the control specimen the first visible crack appeared at a load of about 70 kN. The crack extended from the point of loading to the support in the weak side. As loading progressed, the crack widened, and another major crack appeared in addition to several minor ones as seen in Figure 10. The specimen failed at a load of 100 kN. Although the failure was brittle it was less sudden than in the case of the other specimens

##### 3.1.2 Specimen EB

The first visible crack appeared at a load of 78 kN between the sheets. As loading progressed, cracks widened then the specimen finally failed in a brittle manner at a load of 130 kN after debonding started at the second sheet after the support. Then with further loading the failure occurred progressively one sheet at a time.

Post failure examination of the specimen showed a similar crack pattern to the control specimen as seen in Figure 11. It was noticed that the bonding failure took place in the concrete thin layer adjacent to the sheet, not in the adhesive epoxy.



Figure 11 Failure and crack pattern of specimen EB

##### 3.1.3 Specimen NSM

The first visible crack appeared at a load of 80 kN. Discontinued small cracks appeared between the strips as the loading progressed. The specimen failed suddenly in an explosive manner at a load of 155 kN, as the concrete cover containing the strips debonded from the beam's inner core as seen in Figure 12. After removing the concrete cover a similar crack pattern to the control specimen could be seen in the concrete core as seen in Figure 13. It was noticed that no de-bonding occurred between the CFRP laminates and the concrete.

##### 3.1.4 Specimen IER-G

The first visible crack appeared at a load of 70 kN at the loading point at a steeper angle than in the case of the control specimen. This can be related to the crack arresting action of the embedded bars which altered the cracking pattern compared to the control specimen.



Figure 12 Failure of specimen NSM



Figure 13 crack pattern of specimen NSM

Several other cracks appeared and widened as the loading progressed, although at steeper angle as seen in Figure 14. Failure occurred suddenly at a load of 160 kN due to the de-bonding at the thin layer of concrete adhered to the GFRP bars. No de-bonding between the GFRP bars and the epoxy adhesive was observed and a thin concrete layer was noticed to be fully attached to the GFRP bar as seen in Figure 15.



Figure 14 Crack pattern of specimen IER-G



Figure 15 GFRP bar after failure of specimen IER-G

### 3.1.5 Specimen IER-C

Specimen IER-C behaved in a similar manner to specimen IER-G where the cracks occurred in a steeper form than the control specimen. However, the specimen failed suddenly in a brittle manner at a load of 138 kN. It can be seen that this specimen failed 14 % lower than IER-G. After removing the concrete cover, it was noticed that the beam failed due to the de-bonding action of CFRP bars. On the contrary from the IER-G specimen the de-bonding took place between the bar's coating and its inner fiber core not in the thin concrete layer adjacent to the CFRP bar. This can be related to a manufacturing weak bond between the fiber core and its friction cover as seen in Figure 16.



Figure 16 CFRP bar after failure of specimen IER-C

### 3.2 Deflection behavior

Figure 17 shows the mid-span deflection behavior of all specimens. From this figure it can be concluded that the load-deflection behavior of all tested beams seemed similar up to the maximum load. This means that the stiffness of the beams seemed not to be affected by any type of shear strengthening. This can be due to the use of the same main reinforcement configuration and beam cross section for all the tested beams which governs the flexural behavior. This means that the flexural behavior governed the mid-span deflection behavior and the shear strengthening did not affect this behavior. The figure shows a softening behavior for the control specimen and this is consistent with the less brittle fracture behavior of the control beam compared to the other strengthened beams. All the other four beams failed catastrophically in brittle manner and the failure was explosive, which hindered capturing the post peak behavior in some specimens and only allowed recording two or three points in the softening part of the curve.

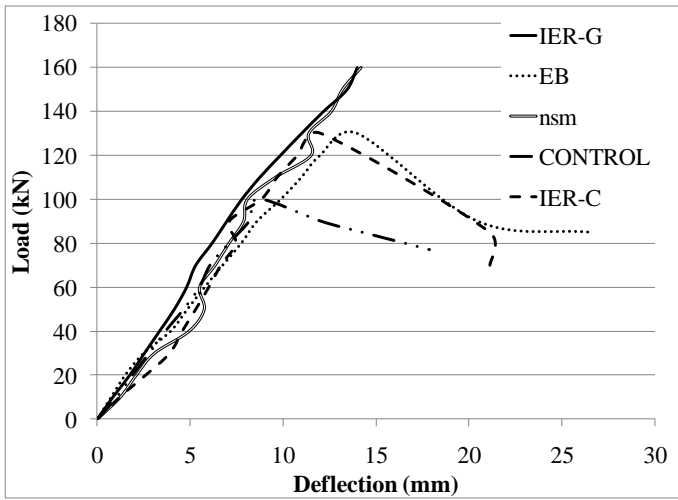


Figure 17 Deflection behavior

### 3.3 Strain behavior

#### 3.3.1 Steel stirrups

Figure 18 shows the load vs. strain in the second stirrup after the support. It can be seen that the strain in the stirrup for the control sample started to pick up the stirrup's load at an early loading stage and the rate of strain increase was much higher than all the other strengthened beams. On the other hand it is apparent from this figure that the stirrups for all the shear strengthened specimens were not activated at small loads until cracking started occurring, after which the stirrups were activated and strain increased. Also it can be noticed that both the strengthened specimens using drilled method IER-C and IER-G had much lower stirrup strain compared to the other strengthened and control specimens, which indicate that the CFRP bars and GFRP bars carried most of the shear forces than its stirrups, this is due to the higher modulus of elasticity of FRP bars compared to the steel stirrups

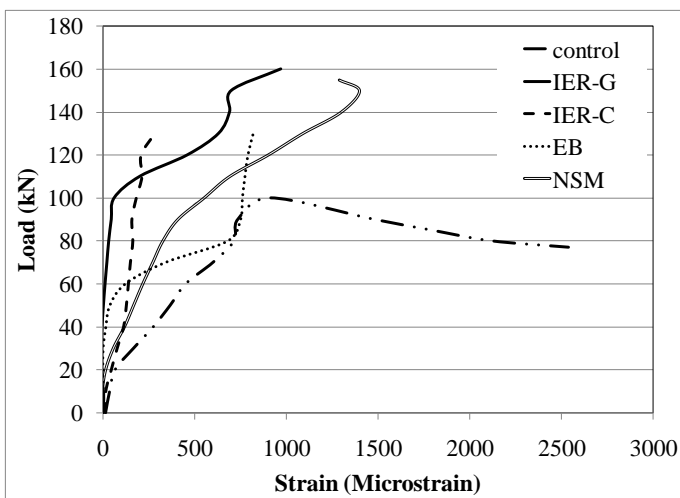


Figure 18 Steel stirrup strain behavior

#### 3.3.2 Concrete strains

Figure 19 shows the load vs. concrete strains for control specimen and specimens NSM and EB. The figure shows that the control specimen had a gradual increase in the strain rate as the loading progressed beyond about 18 kN. The higher value of concrete strain for the control specimen is due to cracks forming in the measuring range of the strain gauge.

On the other hand, the other two specimens had an almost similar stiffness to each other until about 75 to 80% of their failure load. The strains in the concrete at failure for these specimens were much smaller than that of the control specimen. This may be related to the change in crack pattern for those strengthened specimens that lead the crack to move away from the measuring range of the strain gauge

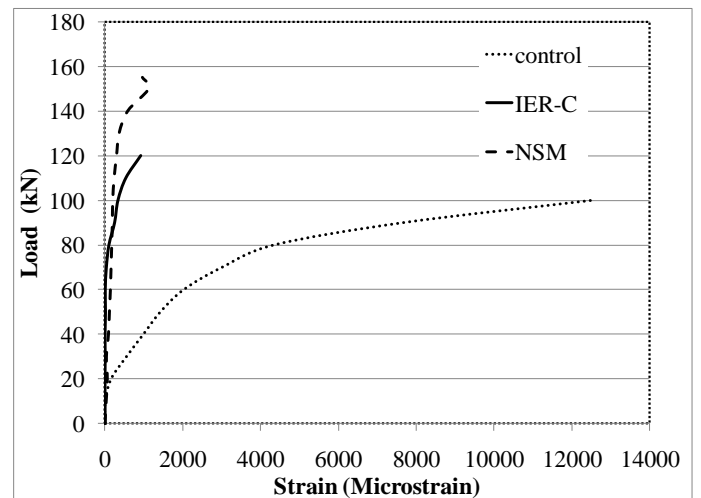


Figure 19 Concrete strain behavior

#### 3.3.3 Strains in strengthening FRP materials

Figure 20 shows the load vs. strain in the second sheet for specimen EB. The sheets seemed not to be activated until the load reached about 40 kN. The strains then increased at a high rate until about 120 kN where debonding started occurring and the strains dropped dramatically.

Figure 21 shows the load vs. strain for the second strip for specimen NSM. The FRP material seemed to be activated at the start of the test and the rate of strain increase seemed to be constant until the concrete cover de-bonding started to occur prior to failure.

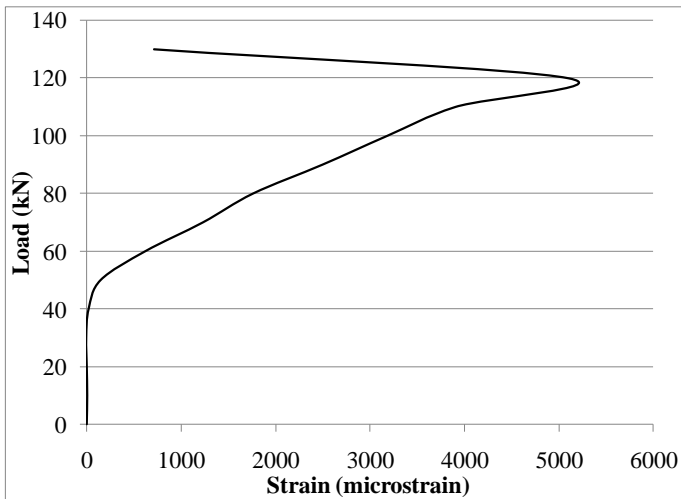


Figure 20 Strain behavior of CFRP sheet in specimen EB

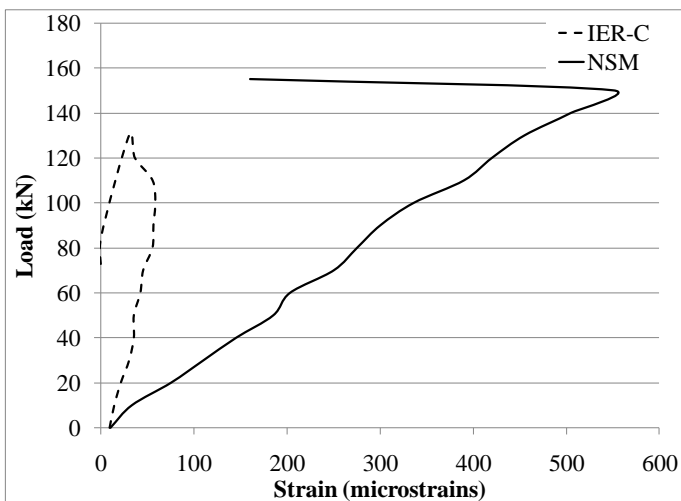


Figure 21 FRP strain behavior of specimens IER-C and NSM

## 4 DISCUSSION OF RESULTS

The test results show that the load at which the first crack appeared was not affected by the IER strengthening technique, and was slightly increased when the beam was externally reinforced by the EB and the NSM techniques. Visual observation of the specimens during testing showed that the EB and the NSM techniques covered or prevented surface cracks from appearing. This could be also concluded from the small strains on the concrete surface compared to the control specimen (Fig. 19). For the IER technique on the other hand surface cracks were more visible, this in some situations is more desirable as it provides a warning of imminent failure or the existing of an overload.

The test results have also shown that all shear strengthening techniques significantly enhance the shear capacity of the beams. The NSM and the IER techniques provide better results than the EB technique. It is worth noting that for the same amount of strengthening material, two grooves at the sides of the beam had to be cut at a spacing of 75 mm for the

NSM technique versus drilling one hole at the center of the beam every 150 mm in the IER technique. Although the use of CFRP reinforcement for IER strengthening yielded a smaller increase in the shear capacity this was due to the de-bonding between the coating and the internal fiber core of the bar. Therefore by enhancing the manufacturing technique for the CFRP and increasing the bond strength between the fiber core and the friction coating, the IER-C technique will yield at least the same shear strengthening capacity as the IER-G technique. This means also that a different surface treatment for the CFRP bar may produce better strengthening capacity. It is worth noting that the use of GFRP bars for this technique, which are more economical, yielded slightly better results than the NSM technique and had a 50% more strength enhancement over the EB technique.

## 5 CONCLUSIONS AND FUTURE WORK

Based on the results of this experimental program the following conclusions and recommendations for future work could be made;

- Using internally embedded FRP reinforcement IER for strengthening RC beams in shear is feasible.
- Using the internally embedded strengthening technique can provide the same strength enhancement as the NSM technique and twice that of the EB technique.
- Using external strengthening techniques prevents or hides surface cracks while for the IER technique surface cracks are more visible.
- The IER technique yields an enhancement in the shear strength equal to in one case and double in another to the EB technique, and equivalent to the NSM technique in one case.
- Further research is needed to study the de-bonding behavior of IER and the effects of the different parameters like the bonding agent, angle of inclination of the IER, the spacing between the IER ...etc. on its behavior.

## 6 REFERENCES

- Barros, J.A.O. & Dias, S.J.E. 2006. Near surface mounted CFRP laminates for shear strengthening of concrete beams. *Cement & Concrete Composites*. 38: 276-292.
- De Lorenzis L & Teng J.G. 2007. Near-surface mounted FRP reinforcement: an emerging technique for structural strengthening. *Composites: PartB*. 38(2):119-143.
- De Lorenzis L, Nanni A. 2001. Shear strengthening of reinforced concrete beams with NSM fiber-reinforced polymer rods. *ACI Structural Journal*. 98(1):60-68.
- Dias, S.J.E. & Barros, J.A.O. 2010. Performance of reinforced concrete T beams strengthened in shear with NSM CFRP laminates. *Engineering Structures*. 32: 373-384.

- Rizzo, A & De Lorenzis, L. 2009. Behavior and capacity of RC beams strengthened in shear with NSM FRP reinforcement. *Construction and Building Materials* 23: 1555-1567.
- Tanarslan, H.M. 2011. The effects of NSM CFRP reinforcements for improving the shear capacity of RC beams. *Construction and Building Materials* 25: 2663-2673.